

# High surface area porous silicon carbide synthesized via sol-gel and carbothermal reduction process

DONG-HUA WANG<sup>a</sup>

<sup>a</sup>Department of Chemistry and Chemical Engineering, Weinan Teachers University, Weinan 714000, PR China

A modified sol-gel method is proposed for the preparation of high surface area porous silicon carbide. In this method, furfuryl alcohol and tetraethoxysilane were used respectively as carbon and silicon precursors for preparing a carbonaceous silica xerogel. Polymethylhydrosiloxane (PMHS) was employed as pore-adjusting agent in the sol-gel process. SiC was obtained by the carbothermal reduction of the carbonaceous silica xerogel at 1300 °C in argon flow and then purified by removing excess silica, carbon and other impurities. XRD, FTIR, SEM, HRTEM and BET were used to characterize the SiC samples. The results show that the SiC products are found to have high specific surface area of 167 m<sup>2</sup>/g. PMHS has important effect on the surface area, pore volume of the SiC products. The SiC exhibits different photoluminescence properties.

(Received March 3, 2011; accepted March 16, 2011)

**Keywords:** Sol-gel, Polymethylhydrosiloxane, High surface area silicon carbide, Carbothermal reduction, XRD, FTIR, SEM, HRTEM, BET

## 1. Introduction

Due to their excellent performances, such as low density, high permeability, and high specific surface areas, porous materials have found numerous applications, including filters, catalyst supports, sensors, separations, and tissue engineering [1, 2]. Porous silicon carbide materials are potential candidates for such applications due to their excellent thermal and chemical stability [3]. However the low surface area has limited the application of SiC as a catalyst support, therefore many efforts have been done on the synthesis of high surface area SiC in recent years [4-9]. Jin et al. proposed a modified sol-gel method for the preparation of mesoporous SiC [6]. In the method, tetraethoxysilane (TEOS) and phenolic resin were used for preparing binary carbonaceous silicon xerogels, and nickel nitrate was employed in the sol-gel process as catalyst. The carbothermal reduction of the xerogels produced porous SiC with a surface area of 112 m<sup>2</sup>/g. Lu et al. reported mesoporous SiC with surface area of about 160 m<sup>2</sup>/g via nanocasting and carbothermal reduction process. In their method mesoporous silica, SBA-15, was used as nanoreactor, and furfuryl alcohol as carbon source [7]. Keller et al. prepared  $\beta$ -SiC with a high surface area (140 m<sup>2</sup>/g) by the Shape Memory Synthesis (SMS) method [8]. Zheng et al. also reported a kind of high surface area silicon carbide prepared by dynamic vacuum carbothermal reduction [9]. Most preparation methods mentioned above exploit the diversity of carbon and silicon precursors, and synthetic conditions, while a few reports make use of hard templates [7]. Soft templates seldom used for the preparation of porous SiC since the porous structures resulted from soft templates will be destroyed at temperatures far below those for producing SiC [10]. Therefore, it is interesting to investigate the application of soft templates in the preparation of high surface area SiC.

Polymethylhydrosiloxane (PMHS), as a silicon industry by-product, is cheap, nontoxic and stable in air and moisture. Recently, it has been used as structure-directing agent in the preparation of mesoporous silica materials [11]. Here, we employed PMHS as soft templates in the preparation of carbonaceous silica xerogels. In the EtOH system, PMHS molecules can assemble themselves into helices in the sol-gel process and thus lead to the formation of porous structure in the xerogels. The obtained SiC can partly inherit the porous structure from its xerogel precursors in the carbothermal reduction, and thus have large surface area and pore volume.

## 2. Experimental

All the chemical agents were used as received without further purification. Polymethylhydrosiloxane (PMHS) (99%, Mw 2700–5400) was supplied by Acros. Tetraethoxysilane (TEOS, 99%), ethyl alcohol (anhydrous), furfuryl alcohol (99%) and ethylenediamine (99%) were provided by Tianjin chemical corporation.

The synthesis process includes the preparation of a carbonaceous silica xerogel and subsequent carbothermal reduction of the xerogel. The xerogel preparation is briefly described as follows. Firstly, 30ml of PMHS was mixed with 30 ml of furfuryl alcohol and 180 ml of ethanol under stirring. The resultant solution was further stirred for 24 h at room temperature in order that PMHS can react with ethanol and release hydrogen under the catalysis of ethylenediamine (1ml). Secondly, 18 ml of deionized water and 1 g of cobalt nitrate were added into the mixture under vigorous stirring. Afterwards, 50 ml of tetraethoxysilane was added into the above mixture to form a sol. After 24 h, 1 ml of ethylenediamine solution was added into the sol to enhance its gelation. Finally, the gel was dried at 110 °C for 12 h to obtain a carbonaceous

silica xerogel. In this case, the xerogel had a PMHS/TEOS volume ratio of 1/2, and therefore it was denoted as X0.6.

The carbothermal reduction was carried out in a horizontally tubular reactor. The xerogels were heated at 1300 °C in argon flow and maintained at the temperature for 7 h. The raw products were collected after the furnace was cooled down to room temperature, and then purified by air calcination at 700 °C for 2h to remove unreacted carbon followed by acid treatment with HF and HCl (volume ratio of 3/1) for 48h to eliminate the impurities. The purified samples were denoted as SiC-X0.6.

The crystalline phases of the samples were analyzed by a Rigaku D-Max/RB X-Ray diffractometer (XRD) with CuK $\alpha$  radiation. The morphology was examined by LEO-438VP scanning electron microscope (SEM). The microstructures of the samples were characterized by JEM-2010 high-resolution transmission electron microscope (HRTEM). The BET surface area, pore volume and pore size distribution of the samples were determined from corresponding nitrogen adsorption-desorption isotherms (at 77 K) by using a Micromeritics ASAP-2000. Surface areas were calculated from the linear part of the BET plots according to the IUPAC recommendation. Pore size distributions of the samples were calculated via the BJH model. The FTIR datas were collected using a Nicolet 470 FTIR spectrometer operating at a resolution of 4 cm $^{-1}$ .

### 3. Results and discussion

The sample is greenish powders. XRD analysis showed that SiC-X0.6 is  $\beta$ -SiC, and no other crystalline phases such as silica, carbon or other impurities were detected. The widths and intensities of the diffraction peaks in the XRD patterns are related to the average particle size of the samples, and they are often used to estimate the particle size. The sample gives wider and less intense diffraction peaks as shown in Fig. 1, indicates that the sample consists of smaller particles. For the present SiC sample, however, no diffraction peak can be found from the XRD pattern in the low-angle region. This indicates that the structure of the SiC sample is disordered.

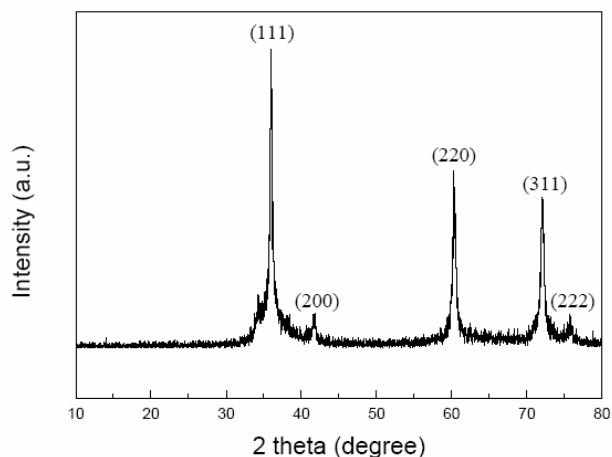


Fig. 1 XRD patterns of the SiC samples.

The SEM image of SiC-X0.6 is shown in Fig. 2a. It is seen that the sample mainly consists of irregular particles with sizes from 1 to 50  $\mu$ m. However, the irregular particles consist of small particles with sizes of tens to hundreds nanometers, as shown in Fig. 2b. To investigate the structural features of these irregular particles, the sample was further observed by HRTEM, as shown in Figs. 2c and 2d. From the images, the particles have irregularly porous structures with the pore diameters from 10 to 50 nm. Fig. 2d reveals that the pore walls are crystalline, and gives the arrangement of atomic layers. The measured distance between two adjacent lattice fringes is 0.25 nm, which corresponds well to the interplanar spacing of the (111) plane of  $\beta$ -SiC. These results indicate that the SiC-X0.6 has porous structures.

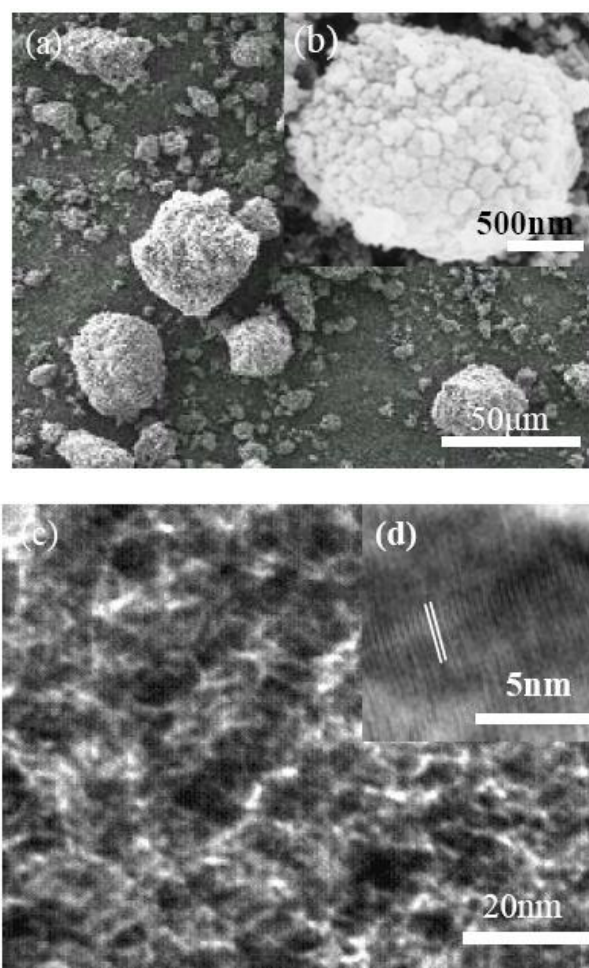


Fig. 2 SEM image of SiC-X0 (a), SEM image of SiC-X0.6 (b), TEM image of SiC-X0.6 (c), and HRTEM lattice image of the SiC-X0.6 (d).

Fig.3a shows the low-temperature nitrogen adsorption-desorption isotherms and the pore size distributions of the SiC-X0.6. The isotherms exhibit an abrupt change in the relative high  $P/P_0$  range (0.6-0.9), indicating that the samples possess large nanopores [12]. The Barret-Joyner-Halenda (BJH) method was employed to calculate the pore size distributions of SiC sample [13].

From the calculation results, the sample has wide pore size distribution. This indicates that the pores in the SiC samples are disordered, which are in agreement with the TEM result shown in Fig. 2c.

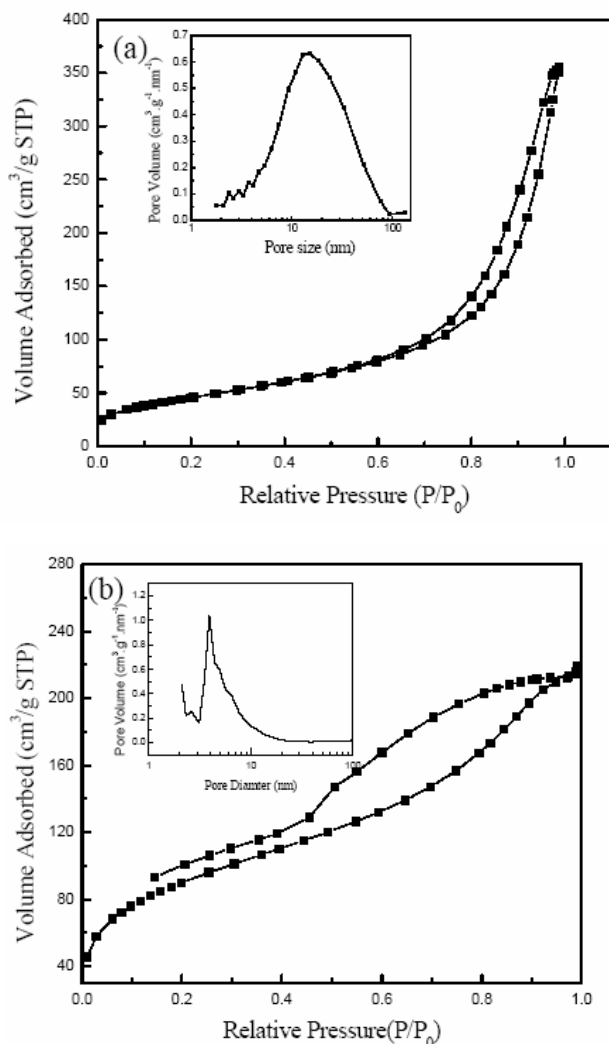


Fig. 3 Nitrogen-desorption isotherms and pore-size distributions (insets) of SiC samples: (a) SiC-X0.6 and (b) X0.6.

Fig. 3b shows the  $N_2$  adsorption–desorption isotherms and the pore size distributions of xerogel X0.6. The results indicate that the xerogel X0.6 has mesoporous structures. However the hysteresis loops of the xerogel at low  $P/P_0$  values ( $<0.2$ ) is not closed. This is due to the existence of organic functional groups and the effect of pore connectivity [14]. The textural parameters of SiC-X0.6 and xerogel X0.6 are summarized in Table 1.

Table 1 Nitrogen adsorption results of the SiC-X0.6 and X0.6.

samples	surface area ( $m^2/g$ )	pore volume ( $cm^3/g$ )	peak pore size (nm)
SiC-X0.6	167	0.55	13
X0.6	329	0.34	4

The FTIR technique was employed to determine the existence of PMHOS in the xerogels. From Fig. 4, the stretching band at  $2974\text{ cm}^{-1}$  and deformation band at  $1384\text{ cm}^{-1}$  of methyl group, the deformation band at  $1274\text{ cm}^{-1}$  of the silicon-bonded methyl group, and the Si-C stretching band at  $773\text{ cm}^{-1}$  can be observed in the FTIR spectrum of X0.6. These confirm that the methyl group ( $-CH_3$ ) in the xerogel is still bonded to the silica framework. The band at  $2170\text{ cm}^{-1}$  is the characteristic adsorption of Si-H, indicating that there still exists a little Si-H bond in the xerogel. The wide band at about  $3440\text{ cm}^{-1}$  can be ascribed to the association vibration of O-H bond in Si-OH, and it means the formation of PMHOS.

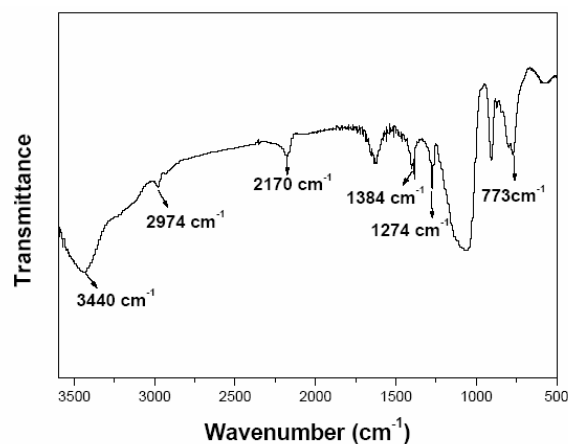


Fig. 4 FTIR spectra of X0.6.

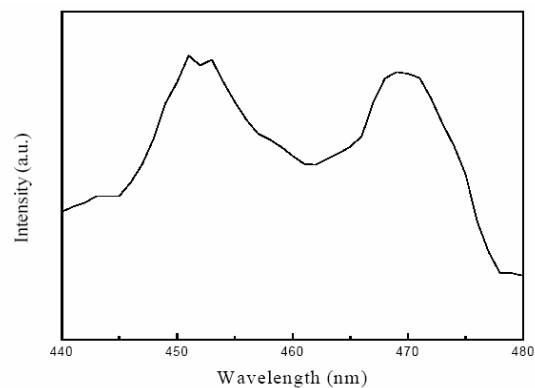
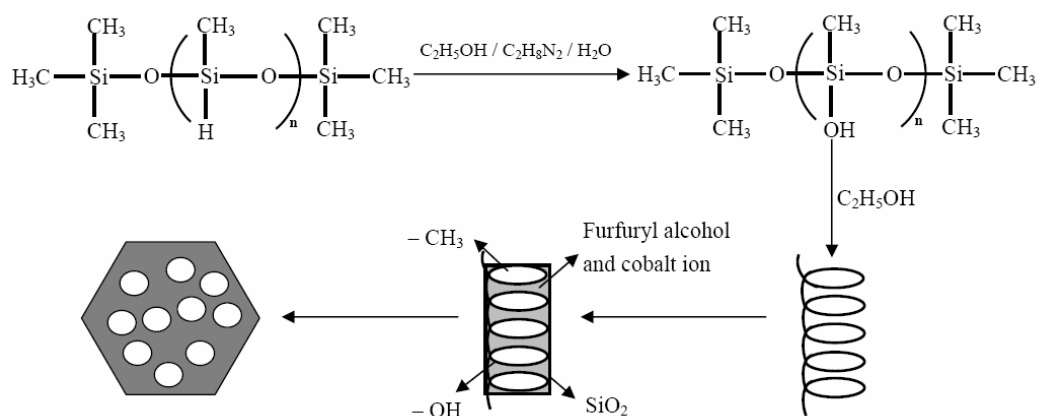


Fig. 5. PL spectrum of SiC-X0.6.

The porous structures in the SiC samples are related to the special structure of PMHS. In the presence of ethylenediamine as catalyst, the active hydrogen in PMHS can be replaced by hydroxy groups, and this can result in the conversion of PMHS to PMHOS, in which hydrophobic and hydrophilic groups appear in the whole molecular chain [15]. In the EtOH system, long-chain like PMHOS molecules assemble themselves into a helical structure with several loops whose both sides are occupied by hydroxy and methyl groups, respectively. The methyl groups are arranged inside the loops because of their

hydrophobic trait and the hydrophilic hydroxys are outside the loops [11]. Hydrophilic furfuryl alcohol molecules and cobalt ions will surround the hydroxys to fill the hole between PMHS loops. After adding TEOS in the system, TEOS reacts with the hydroxys outside the loops. As a result, these loops are fixed at molecular scale and the regions inside the loops form the mesopores in the xerogels. The pores are disordered due to the irregular arrangement of PMHS helices. The above processes can be illustrated in Scheme 1.



Scheme 1 The pore formation from spiral PMHOS configuration in EtOH system.

In the present work, cobalt component in the xerogels also acts as catalyst during the carbothermal reduction. First, metallic cobalt particles are formed from decomposition of cobalt nitrate. Subsequently melted cobalt particles react with silica and produce various cobalt silicide active phases. The active phases exist between the C-SiO<sub>2</sub> interface and absorb carbon and silica to produce SiC [16]. The reaction may occur between the carbon and silica on the loop, therefore the helical framework can be partly kept. With the reaction proceeding, the SiO<sub>2</sub> layers outside the loops will be changed into SiC, which forms the porous SiC framework.

Porous structures of SiC can influence their physical properties. The photoluminescence (PL) spectrum of the high surface area porous SiC nanowires is depicted in Fig.5. The PL spectrum consists of two peaks at 450 nm and 470 nm respectively. The peak at 450 nm is similar to the result for 3C-SiC hollow spheres [17]. This indicates that the sample has a size-confinement effect similar to SiC hollow spheres. The peak at 470 nm is close to that of SiC nanotubes [18]. This phenomenon indicates that the luminescence characteristic depends strongly on the SiC nanostructure, which is affected by the synthetic variables such as the materials used, reaction temperature, and the synthetic route of reaction.

#### 4. Conclusions

A novel sol-gel route was presented to prepare porous  $\beta$ -SiC with high specific surface area. In the present method, polymethylhydrosiloxane (PMHS) was employed as soft templates in the sol-gel processes to get binary carbonaceous silicon xerogels. The special structure of PMHS can lead to the formation of porous structures in the xerogel, which could be kept during the carbothermal reduction process. The high surface area SiC exhibits different photoluminescence properties. The present route can be regarded as a convenient method for the preparation of porous SiC, a prospective material for catalyst support.

#### Acknowledgements

The authors acknowledge the financial support from Natural Science Basic Research Plan in Shaanxi Province of China (Program No. 2010JQ6014) and the Special Post-graduate Research Projects of Weinan Teachers University (No.10YKZ051).

**References**

- [1] R. A. Caruso, J. H. Schattka, *Adv. Mater.*, **12**(24), 1921 (2000).
- [2] Y. J. Wang, F. Caruso, *Adv. Funct. Mater.*, **14**(10), 1012 (2004).
- [3] V. G. Pol, S. V. Pol, A. Gedanken, S. H. Lim, Z. Zhong, J. Lin, *J. Phys. Chem. B*, **110**(23), 11237 (2006).
- [4] N. Keller, C. Pham-Huu, S. Roy, M. J. Ledoux, C. Estournes, J. Guille, *J. Mater. Sci.*, **34** (13), 3189 (1999).
- [5] F. Cheng, S. M. Kelly, F. Lefebvre, S. Clark, R. Supplit, J. S. Bradley, *J. Mater. Chem.*, **15**(7), 772 (2005).
- [6] G. Q. Jin, X. Y. Guo, *Micropor. Mesopor. Mater.*, **60**(1-3), 207 (2003).
- [7] A. H. Lu, W. Schmidt, W. Kiefer, F. Schuth, *J. Mater. Sci.*, **40**(18), 5091 (2005).
- [8] N. Keller, O. Reiff, V. Keller, M. J. Ledoux, *Diam. Relat. Mater.*, **14**(8), 1353 (2005).
- [9] Y. Zheng, Y. Zheng, R. Wang, K. M. Wei, *J. Mater. Sci.*, **43**(15), 5331 (2008).
- [10] M. Kamperman, C. B. W. Garcia, P. Du, H. S. Ow, U. Wiener, *J. Am. Chem. Soc.*, **126**(45), 14708 (2004).
- [11] D. J. Yang, J. P. Li, Y. Xu, D. Wu, Y. H. Sun, H. Y. Zhu, F. Deng, *Micropor. Mesopor. Mater.*, **95**(1-3), 180 (2006).
- [12] K. S. W. Sing, D. H. Everett, R. A. W. Haul, L. Moscou, R. A. Pierotti, J. Rouquerol, T. Siemieniowska, *Pure Appl. Chem.*, **57**(4), 603 (1985).
- [13] E. P. Arrett, G. Joyner, P. P. Halenda, *J. Am. Chem. Soc.*, **73**(1), 373 (1951).
- [14] X. J. Zhang, T. Y. Ma, Z. Y. Yuan, *Eur. J. Inorg. Chem.*, **17**, 2721 (2008).
- [15] N. J. Lawrence, M. D. Drew, S. M. Bushell, *J. Chem. Soc., Perkin Trans*, **1**(23), 3381 (1999).
- [16] X. Y. Guo, G. Q. Jin, *J. Mater. Sci.*, **40**(5), 1301 (2005).
- [17] G. Z. Shen, D. Chen, K. B. Tang, Y. T. Qian, S. Y. Zhang, *Chem. Phys. Lett.*, **375**(1-2), 177 (2003).
- [18] J. Q. Hu, Y. Bando, J. H. Zhan, D. Golberg, *Appl. Phys. Lett.* **85**(14), 2932 (2004).

---

\*Corresponding author: wangdongh1978@163.com